MedChemComm

Accepted Manuscript

ROYAL SOCIETY OF CHEMISTRY

www.rsc.org/medchemcomm

THE SYNTHESIS AND FUNCTIONAL EVALUATION OF A MITOCHONDRIA TARGETED HYDROGEN SULFIDE DONOR, 10-OXO-10-(4-(3-THIOXO-3*H*-1,2-DITHIOL-5-YL) PHENOXY) DECYL) TRIPHENYLPHOSPHONIUM BROMIDE (AP39)

Sophie Le Trionnaire[a], Alexis Perry[b], Bartosz Szczesny[c], Csaba Szabo[c], Paul G. Winyard[a], Jacqueline L. Whatmore[a], Mark E. Wood[b] & Matthew Whiteman[a]**

Received (in XXX, XXX) Xth XXXXXXXXX 200X, Accepted Xth XXXXXXXXX 200X
First published on the web Xth XXXXXXXXX 200X
DOI: 10.1039/b00000000x

Synthesis and bioavailability of the endogenous gasomediator hydrogen sulfide (H_2S) is perturbed in many disease states, including those involving mitochondrial dysfunction. There is intense interest in developing pharmacological agents to generate H_2S. We have synthesised a novel H_2S donor molecule coupled to a mitochondria-targeting moiety (triphenylphosphonium; TPP^+) and compared the effectiveness of the compound against a standard non-TPP^+ containing H_2S donor (e.g. GYY4137) in the inhibition of oxidative stress-induced endothelial cell death. Our study suggests mitochondria-targeted H_2S donors are useful pharmacological tools to study the mitochondrial physiology of H_2S in health and disease.

1 Introduction

Hydrogen sulfide (H_2S) is now convincingly established as the third gasotransmitter,[1-3] alongside the more familiar nitric oxide (NO) and carbon monoxide (CO). It is enzymatically produced from amino acids cysteine, homocysteine and cystathionine by two pyridoxal-5'-phosphate-dependent enzymes, namely cystathionine-γ-lyase (CSE) and cystathionine-β-synthase (CBS).[1-3] A third α-ketoglutarate and cysteine-dependent enzyme, located in the mitochondria of cells, 3-mercaptopyruvate sulfurtransferase (3-MST)[4] has also been proposed to generate H_2S within the mitochondria[5].

In the vascular system, H_2S has been proposed as an endothelium-derived vasodilator and genetic knock-out of CSE in animals results in hypertension[6] and accelerates atherosclerosis[7]. Similarly, decreased H_2S biosynthesis and/or bioavailability have been observed in various human disease states (and animal disease models)[1-3] including those with marked mitochondrial and endothelial dysfunction and oxidative stress such as hypertension, diabetes, obesity[8], pre-eclampsia[9] and after myocardial infarction[10]. Collectively, these studies have highlighted the therapeutic potential of pharmacological strategies to increase H_2S bioavailability in these pathologies.

There is extensive evidence for a role of oxidative stress, and the over-production of detrimental oxidants, in the vascular endothelium of several human disease states including diabetes, obesity, hypertension and stroke[11]. Oxidant species such as peroxynitrite, ($ONOO^-$) and hydrogen peroxide (H_2O_2), as well as the products of biomolecule oxidation such as the lipid-derived aldehyde 4-hydroxynonenal (4-HNE), are well known to induce endothelial and mitochondrial dysfunction and cell death[11].

Mitochondria are key intracellular organelles determining cell fate (survival and death) and they are a key source (and target) for detrimental oxidant production within cells[12]. As such, compounds that can 'target' mitochondria and prevent or limit mitochondria-mediated oxidative stress have received considerable attention and lipophilic cations such as triphenylphosphonium (TPP^+) have been extensively used for this purpose[13]. TPP^+ derivatives are extensively and rapidly taken up by mitochondria *in vivo*, due to the large negative membrane potential inside the mitochondria ($\Delta\psi m$), resulting in the high concentration of the TPP^+-derivatives within the mitochondria[13]. The covalent attachment of the lipophilic TPP^+ cation has become established as a generic and robust method for selectively delivering small, bioactive molecules to mitochondria *in vivo*.[13]

H_2S donor compounds such as GYY4137 **1** (Fig. 1)[14] have been shown to exert prominent vasodilatory activity *in vitro*[14,15] and in hypertensive animals *in vivo*[9,14,15]. GYY4137 **1** also inhibited inflammatory signalling in *in vitro*[16-19] and *in vivo* models of sepsis[18], arthritis[20], pre-eclampsia[9] and atherosclerosis[21]. Furthermore, GYY4137 has also been shown to inhibit oxidative stress-mediated cytotoxicity and loss of mitochondrial function induced by H_2O_2, $ONOO^-$ and 4-HNE[22]. However, GYY4137 is highly water soluble[14], limiting its cellular permeability, and the above studies have all used high concentrations of GYY4137 (≥100 μM) for anti-inflammatory, vasodilatory, cytoprotective and mitochondrial protective effects to be seen. The need for such high concentrations may further limit its therapeutic potential and alternative strategies for generating potent H_2S donor molecules would be useful.

Dithiolethiones, such as **2**, have been proposed as novel species for H_2S delivery (reviewed in[23]) (Fig. 1) and dithiolethione derivatives of non-steroidal anti-inflammatory drugs (e.g. naproxen, diclofenac, indomethacin) have been clearly shown to generate H_2S *in vivo*, promote gastro-intestinal blood flow and prevent gastric injury *in vivo* and exert prominent anti-inflammatory effects with marked additional pharmacological benefit over the parent NSAID alone[23-28].

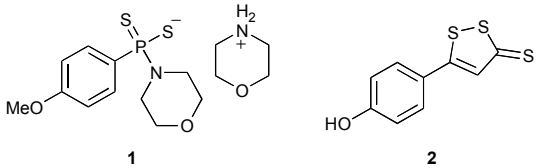

1 **2**

Fig. 1 H_2S donors; GYY4137 **1**, 5-(4-Hydroxyphenyl)-3*H*-1,2-dithiole-3-thione **2**.

Therefore, with the above observations in mind, we have synthesised a TPP^+-derivative of dithiolethione **2** to generate a novel mitochondria-targeted H_2S donor molecule. We have then

evaluated its effects in a cellular model of oxidative stress and compared its efficacy with an established standard H_2S donor, GYY4137 **1**.

2 Results

2.1 Synthesis

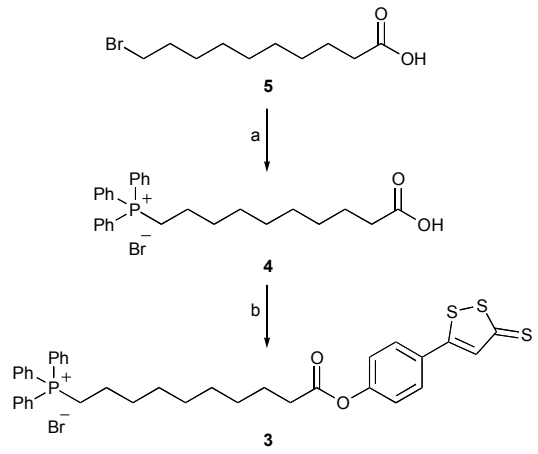

Scheme 1 Preparation of AP39 **3**. *Reagents and conditions*: (a) triphenylphosphine (1.0 equiv.), CH_3CN, reflux, 70 h; (b) 5-(4-hydroxyphenyl)-3*H*-1,2-dithiole-3-thione **2** (1.0 equiv.), *N*,*N*-dicyclohexylcarbodiimide (1.0 equiv.), 4-dimethylaminopyridine (0.05 equiv.), CH_2Cl_2, room temp., 22 h (73% from **5**).

AP39 **3** was prepared in an overall yield of 73% using the two-step process shown in Scheme 1. Phosphonium salt **4** was prepared from 10-bromodecanoic acid **5** and triphenylphosphine under reflux conditions in acetonitrile[33] and coupled, using standard carbodiimide conditions, to 5-(4-hydroxyphenyl)-3*H*-1,2-dithiole-3-thione **2**.[26] Final purification of **3** was achieved using flash chromatography on silica gel (eluting with methanol), the product forming a crisp foam (which could be handled as a solid) on removal of the solvent.

2.2 Intracellular generation of H_2S from AP39

Figure 2 show the generation of H_2S from AP39 **3**, detected using two different fluorescence probes selective for sulfide, WSP-1[29,30] and 7-azido-4-methylcoumarin (AzMC)[31,32]. AP39 induced a concentration-dependent increase in WSP-1 fluorescence, indicative of intracellular H_2S generation[29] in human cerebral microvascular endothelial cells (hCMEC/D3) (Fig. 2A). Furthermore, exposure of B.End3 cells to AP39 **3** (100 nM) for 1 hour resulted in an increase in the fluorescence of an alternative H_2S fluorophore AzMC, with significant co-localisation of the signal to mitochondria (Mitotracker) (Fig. 2B)

2.3 Cytotoxicity

Preliminary control experiments were conducted to confirm that the addition of up to 5 μM AP39 and 2 mM GYY4137 for 24 h did not induce significant cytotoxicity compared with vehicle controls (alamarBlue®; data not shown). Figure 3 shows concentration-dependent (7 – 250 nM) inhibition of oxidative stress-mediated toxicity in hCMEC/D3 cells by AP39 **3** and GYY4137 **1** induced by [A] SIN-1 (500 μM), [B] H_2O_2

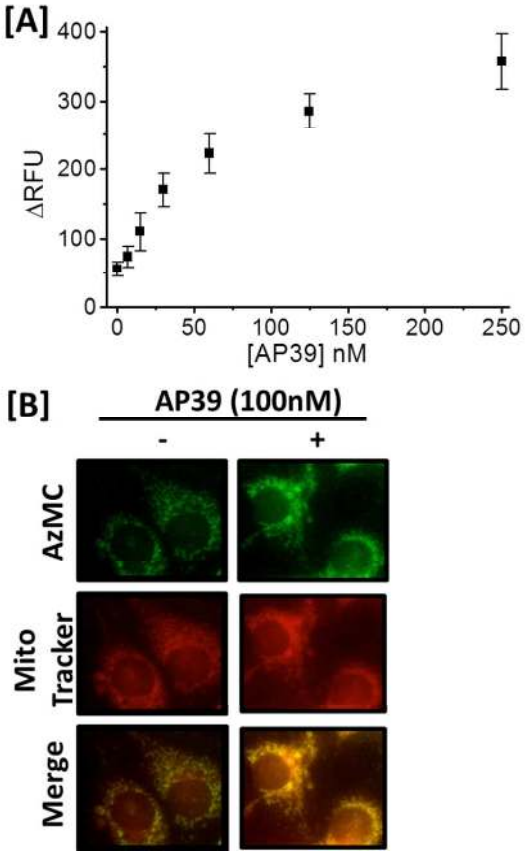

Figure 2: Intracellular generation of H_2S from AP39. Endothelial cells were treated with 7-250 nM AP39 for 1 hour and intracellular H_2S was detected in human hCMEC/D3 cells using WSP-1 [A]. Co-localisation of mitochondria and H_2S was visualised after 1 hour treatment of murine B.End3 cells with AP39 (100 nM) by fluorescence microscopy using MitoTracker Red (for mitochondria) and AzMC (for H_2S) [B]. Images are representative images of three or more independent experiments. Note the concentration-dependent increase in H_2S signal which, at least in part, co-localises within the mitochondrial regions suggesting AP39 generated H_2S mainly in mitochondria.

(50 μM) and [C] 4-HNE (10 μM). The concentration where 50% of cell viability was recovered was estimated to be 25 nM (*vs* SIN-1), 30 nM (*vs* H_2O_2) and >125 nM (*vs* 4-HNE). In order to show that the cytoprotective effects were due to AP39 **3** and not the constituent parts of the AP39 molecule, cells were incubated with 100 nM of the H_2S donor moiety (ADT-OH, **2**), the phosphonium salt containing the mitochondria-targeting motif **4** individually and in combination, and then exposed the cells to SIN-1, H_2O_2 or 4-HNE. Neither ADT-OH **2**, compound **4** (TPP-decanoate) or a 100 nM each of ADT-OH **2** with **4**, induced significant cytoprotection against oxidative stress-mediated cytotoxicity (Figs. 3A-C) confirming that cytoprotection was due to AP39 **3**.

We next compared the efficacy of AP39 **3** against an established H_2S donor compound GYY4137 **1**, which has previously been shown to protect human mesenchymal progenitor cells and articular chondrocytes from oxidative stress-mediated toxicity[22]. Figure 3 also shows that when used at the same concentration as AP39 (7 – 250nM), GYY4137 **1** was not cytoprotective. However, as expected[14-20] significant inhibition of oxidative stress-induced cell death was observed with much higher concentrations (e.g. ≥100 μM) (Fig. 3D). From these studies, concentrations of 100 nM AP39 and 100 μM GYY4137 **1** were used for subsequent experiments.

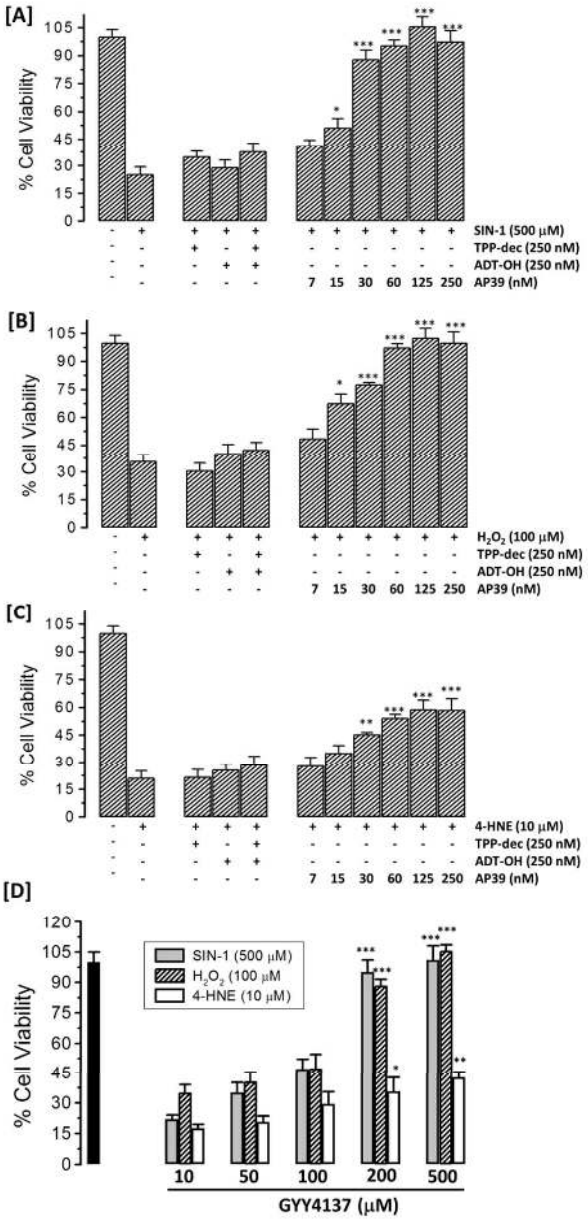

Figure 3: Concentration-dependent inhibition of oxidative-stress induced cell death by AP39 and GYY4137. hCMEC/D3 cells were incubated with increasing concentrations of AP39 **3** and GYY4137 **1** (7-250 nM) for 1 hour and [A] SIN-1 (500 μM), [B] H_2O_2 (50 μM) and [C] 4-HNE (10 μM) added. Higher concentrations of GYY4137 **1** (10 – 500 μM) were also examined [D]. Control experiments were also performed using ADT-OH **2**, compound **4**, alone and in combination [A-C]. Cell viability was assessed by Alamar blue assay after 24 hours. *p<0.05, **p<0.01 and *** p<0.001 H_2S donors *c.f.* oxidant treatment

2.4 Effects of H_2S donors on mitochondrial membrane potential (ΔΨm), ATP and mitochondrial oxidant production

Figure 4 shows AP39 **3** (100 nM) and GYY4137 **1** (100 μM) significantly inhibited oxidative stress-induced loss of mitochondrial membrane potential (Fig. 5A) and inhibited mitochondrial production of reactive oxygen species, detected using mitosox red (Fig. 4B). Incubation of cells with AP39 **3** (100 nM) or GYY417 **1** (100 μM) alone had no significant effect on mitochondrial membrane potential or mitochondrial oxidant production (data not shown).

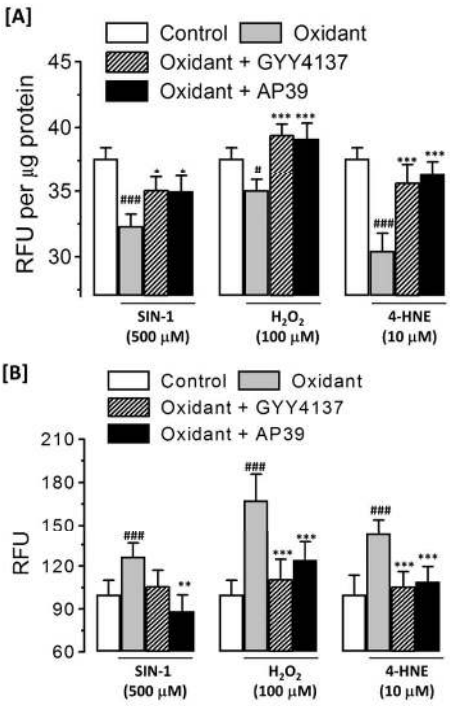

Figure 4: Inhibition of oxidative-stress induced cell toxicity by H_2S donors. Human hCMEC/D3 endothelial cells were incubated with AP39 **3** (100 nM) or GYY4137 **1** (100 μM) for 1 hour prior to the addition of SIN-1 (500 μM), H_2O_2 (50 μM) or 4-HNE (10 μM). After 24 hours, mitochondrial membrane potential [A] was determined using TMRM and mitochondrial oxidant production [B] determined using MitoSox. ###p<0.001 oxidant treated cells *c.f.* control; *p<0.05, ** p<0.01***, p<0.001 H_2S donors *c.f.* oxidant treatment.

Furthermore, AP39 (100 nM) significantly inhibited mitochondrial oxidant production induced by rotenone (5 μM), an inhibitor of mitochondrial respiratory complex I (Fig. 4A) and loss of ATP (Fig. 4B). GYY4137 also prevented rotenone-induced mitochondrial toxicity, albeit when used at a final concentration of 100 μM.

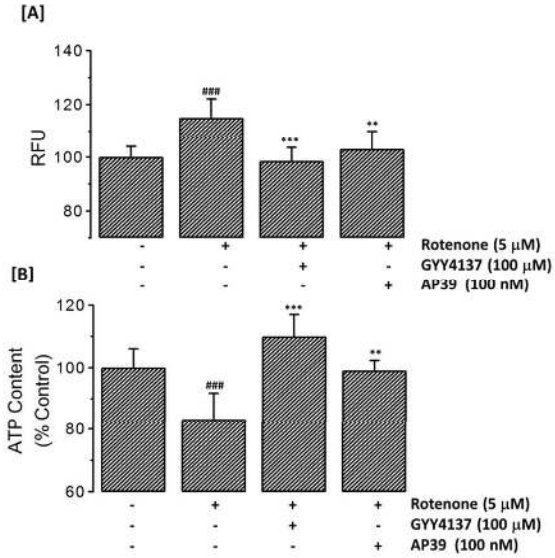

Figure 5: Inhibition of rotenone induced mitochondrial toxicity by H_2S donors. Human hCMEC/D3 endothelial cells were incubated with AP39 **3** (100 nM) or GYY4137 **1** (100 μM) for 1 hour prior to the addition of rotenone (5 μM). Mitochondrial oxidant production was assessed using MitoSox (5 μM) [A] and ATP levels determined using firefly lantern luciferase [B]. ## p<0.01 and ### p<0.001 oxidant treated cells *c.f.* control; **p<0.01, *** p<0.001 H_2S donors *c.f.* oxidant treatment

3 Experimental

3.1 General synthetic chemistry methods

Starting materials and reagents were obtained from commercial suppliers (Sigma-Aldrich and Fisher Scientific) and were used without further purification. Infrared spectra were recorded using a Perkin Elmer Spectrum BX FT-IR spectrometer. Only major absorbances are quoted, using the abbreviations: (for intensity) w, weak; m, medium; and s, strong. Samples were prepared as potassium bromide discs. ^{1}H NMR spectra were recorded at 300 MHz using a Bruker ACF300 spectrometer. Chemical shifts are quoted in ppm relative to tetramethylsilane, the residual solvent peak being used for referencing purposes. Coupling constants are quoted to the nearest 0.5 Hz with peak multiplicities for single resonances being labelled as: s, singlet; d, doublet; t, triplet; m, unresolved multiplet, AA'BB', AA'BB' pattern and br, broad. Where delineation of individual resonances is not possible, the relevant peaks are grouped together (over a chemical shift range) as complex.

^{31}P NMR spectra were recorded at 121 MHz using a Bruker ACF300 spectrometer with external automatic referencing.

^{13}C NMR spectra were recorded at 75 MHz using a Bruker ACF300 spectrometer. Chemical shifts are quoted in ppm relative to tetramethylsilane, the solvent peak being used for referencing. Coupling constants are quoted to the nearest 1 Hz with peak multiplicities being labelled using (where appropriate) the abbreviation: d, doublet.

Mass spectra were recorded by the EPSRC National Mass Spectrometry Service Centre, Swansea, UK, in positive ion electrospray (ES^+) mode.

Analytical thin layer chromatography was carried out using Merck Kieselgel 60 F_{254}, coated on aluminium plates, with visualisation of spots by quenching of u.v. (254 nm) fluorescence or staining with alkaline potassium permanganate solution as appropriate. Silica gel with particle size 40-63 µm was used for flash chromatography. Solvents and reagents were used as supplied commercially by SigmaAldrich and Fisher Scientific without additional purification.

A Büchi R110 Rotovapor was used for the removal of solvents under reduced pressure (*ca* 15 mmHg).

3.2 (10-oxo-10-(4-(3-thioxo-3*H*-1,2-dithiol-5-yl)phenoxy)decyl)triphenylphosphonium bromide (AP39) 3

A solution of 10-bromodecanoic acid 5 (500 mg, 1.99 mmol) in acetonitrile (5 cm^3) was added to a stirred solution of triphenylphosphine (522 mg, 1.99 mmol) in acetonitrile (5 cm^3) and the resulting mixture was heated at reflux for 70 h.[23] After cooling to room temperature and evaporation of the solvent *in vacuo*, the residue was triturated with toluene (2 x 10 cm^3) and dissolved in dichloromethane (30 cm^3). 5-(4-Hydroxyphenyl)-3*H*-1,2-dithiole-3-thione[23,24] **2** (456 mg, 2.02 mmol), *N*,*N*-dicyclohexylcarbodiimide (431 mg, 2.09 mmol) and 4-dimethylaminopyridine (12 mg, 0.10 mmol) were added and the resulting solution was stirred at room temperature for 22 h before filtering through a cotton wool plug and evaporation of the filtrate *in vacuo*. A dichloromethane solution of the residue was loaded onto a silica gel flash chromatography column, which was subsequently eluted with ethyl acetate, followed by methanol. The methanol fractions were combined and evaporated *in vacuo* and a dichloromethane solution of the residue was filtered through a filter paper to remove residual silica gel before evaporation *in vacuo* to give the title compound **3** (1.05 g, 73%) as a crisp, orange foam (Found $[M-Br]^+$ (ES^+) 641.1766, $C_{37}H_{38}O_2PS_3$ requires 641.1766); ν_{max}(KBr disc)/cm^{-1} 2925 (m), 2852 (m), 1754 (m) (C=O), 1599 (w), 1521 (w), 1485 (s), 1437 (s), 1410 (m), 1317 (m), 1278 (m), 1185 (s), 1168 (s), 1112 (s), 1026 (s), 996 (m), 896 (w), 839 (w), 747 (m), 722 (m), 690 (m), 535 (m) and 508 (m); ^{1}H NMR (300 MHz, $CDCl_3$) 7.95-7.65 (17H, m, aryl C(2)*H*, aryl C(6)*H* and phenyl C*H*), 7.42 (1H, s, C*H*C=S), 7.23 (2H, part of AA'BB', J = 8.5 Hz, aryl C(3)*H* and C(5)*H*), 3.85 (2H, m, CH_2P^+), 2.58 (2H, t, J = 7.5 Hz, CH_2C=O), 1.80-1.55 (6H, m, 3 x CH_2) and 1.42-1.19 (8H, m, 4 x CH_2); ^{31}P NMR (121 MHz, $CDCl_3$) 25.7 (P^+); ^{13}C NMR (75 MHz, $CDCl_3$) 214.9 (*C*=S), 183.7 (CH=*C*-S), 171.7 (*C*=O), 153.6 (aryl*C*-O), 135.8 (aryl*C*-C=CH), 134.9 (phenyl*C*-H), 133.6 (d, J = 9 Hz, phenyl*C*-H), 130.4 (d, J = 13 Hz, phenyl*C*-H), 128.9 (C=*C*H-C(S)), 128.1 (aryl*C*-H), 122.9 (aryl*C*-H), 118.3 (d, J = 83 Hz, phenyl*C*-P^+), 34.2 (CH_2C(O)), 30.3 (d, J = 13 Hz, CH_2), 29.0 (CH_2), 28.9 (2 x CH_2), 28.8 (CH_2), 24.6 (CH_2), 23.0 (CH_2) and 22.5 (d, J = 18 Hz, CH_2P^+).

3.4 Morpholin-4-ium-4 methoxyphenyl(morpholino) phospinodithioate (GYY4137)

GYY4137 was synthesised as previously described[14].

3.5 Cell Culture

Human cerebral microvascular endothelial cells (hCMEC/D3) were isolated from human brain and kindly provided by Dr. Pierre-Olivier Couraud, University of Paris Descartes[34-36]. The bEND.3 mouse microvascular endothelial cell line was purchased from the American Type Culture Collection, (ATTC #CRL-2299, Manassas, VA)[37,38].

The vascular endothelium is a prime target for oxidative stress *in vivo* and loss of endothelial function and cell death are observed in cardiovascular diseases such as atherosclerosis, hypertension and diabetes[39,40]. Therefore we used these cells as an *in vitro* model of cellular oxidative stress.

hCMEC/D3 cells were seeded on type I collagen (Sigma, rat tail; dilution 1:30) and cultured in endothelial cell media MV2 (PromoCell; C-22221) with a supplement mix (PromoCell; C-39226) diluted to give fetal bovine serum (2.5%), epidermal growth factor (1.25 ng/ml), basic fibroblast growth factor (2.5 ng/ml), insulin-like growth factor (5 ng/ml), vascular endothelial growth factor 165 (0.125 ng/ml), ascorbate (0.25 µg/ml) and hydrocortisone (0.05 ng/ml). hCMEC/D3 cells constitutively express microvascular endothelial cell makers including von Willebrand factor, CD31 (PECAM-1) and CD105 (endoglin) up to passage 35. Cells used in this current study were between passages 25-34. The commercial bEND.3 mouse microvascular endothelial cell line was cultured as described[37,38]. Murine bEnd.3 cells were maintained in DMEM containing glucose (1g/l) supplemented with 10% fetal bovine serum (10%), non-essential amino acids, (1%) penicillin (100 IU/ml) and streptomycin (100 µg/ml) at 37 °C in 10% CO_2.

3.6 Detection of hydrogen sulfide in living endothelial cells

Cells were seeded in Lab-Tek II chamber coverglass (Nalgen Nunc International) and incubated overnight at 37°C and 10% CO_2 humidified incubator. After attachment, the cells were loaded with 7-azido-4-methylcoumarin (AzMC, SIGMA L511455)[30,31] and MitoTracker Red CMXRos (Invitrogen M7512) fluorogenic dyes at 10 microM and 50 nM final concentration, respectively, for 30

min. Next, 100 nM of AP39 **3** was added with fresh media and cells were further incubated for 1 hour, washed twice with PBS containing calcium and magnesium. 50 µl of PBS was then added to each chamber and micro cover glass was attached. The dye's specific fluorescence was visualized under 40x magnification using Nikon eclipse 80i inverted microscope with Photometric CoolSNAP HQ2 camera and NIS-Elements BR 3.10 software. An additional sulfide-specific fluorophore, WSP-1 (Caymen, 11179-5)[29,30] was used to determine intracellular generation of H_2S. In these experiments, cells were seeded overnight in black 96 well microplates (Nalgen Nunc International) and incubated at 37°C with 10 µM WSP-1 for 30 min[30]. After this time, cells were washed with pre-warmed phenol-red free culture media and AP39 (10 nM – 250 nM) added and WSP-1 fluorescence determined (Ex_{465nm}, Em_{515nm}) using Molecular Devices M2e microplate reader.

3.7 Cytotoxicity assays

To induce oxidative stress, hCMEC/D3 cells were exposed to either H_2O_2 (100 µM), SIN-1 (500 µM) or the lipid aldehyde product of lipid peroxidation *in vivo*, 4-hydroxynonenal (4-HNE; 10 µM) for 24 hours in the presence or absence of H_2S donors GYY4137 **1** (100 µM), AP39 **3** (100 nM), ADT-OH **2** (100 nM) or compound **4** (100 nM). After this time cell viability, as an end point for cytotoxicity, was assessed by alamarBlue® assay (AbD Serotec; #BUF012) according to the manufacturer's instructions. Fluorescence was then determined using a Molecular Devices M2e plate reader (fluorescence; Ex_{540nm} / Em_{612nm}) as described. Data are expressed as % of untreated or vehicle treated cells (% viability).

3.8 Assessment of mitochondrial membrane potential (Δψm)

Mitochondrial membrane potential, (ΔΨm) in whole hCMEC/D3 cells were measured by using the fluorescent potentiometric probe tetramethylrhodamine methyl ester (TMRM; Invitrogen). TMRM is a membrane-permeable cationic fluorophore that electrophoretically accumulates in mitochondria in response to their negative potential and decrease of TMRM fluorescence is indicative of ΔΨm disruption and mitochondrial and cellular toxicity. Cells were incubated with SIN-1 (500 µM), H_2O_2 (100 µM) or 4-HNE (10 µM) in the presence or absence of H_2S donors for 18 h and after this time, cells were incubated for 30 min with TMRM (200 nM), washed with warm (37 °C) phosphate buffered saline (pH 7.4) and TMRM fluorescence (Relative Fluorescence Units; RFU) determined by fluorimetry (Ex_{548nm} / Em_{573nm})[41,42].

3.9 ATP determination

hCMEC/D3 cells were seeded overnight on 24 well plates (Greiner) containing 1.0 ml culture media and treated with the respiratory chain inhibitor rotenone (5 µM), and the oxidants SIN-1 (500 µM), H_2O_2 (100 µM) or 4-HNE (10 µM) in the presence or absence of AP39 (100 nM) or GYY4137 (100 µM) for 18 hours. After this time, cells were washed twice with ice cold phosphate buffered saline (PBS) and lysed with 100 µl of ice- cold trichloroacetic acid (TCA; 10% $^{w}/_{v}$). 5 µl of TCA lysate was then added to 200 µl of arsenite buffer (containing 80 mM $MgSO_4$, 10 mM KH_2PO_4 and 100 mM Na_2HAsO_4, mixed in a 1:1:1 ratio; pH 7.4) followed by 10 µl firefly lantern extract (containing luciferase; Sigma)[41,42]. Emitted light was recorded on a GloMax Jr, (Promega) luminescence detector as described. ATP concentrations were determined using a freshly prepared standard curve and samples normalised to cellular protein content using a commercial bicinchoninic acid-based kit (Bio-Rad).

3.10 Intracellular oxidant production

hCMEC/D3 cells were treated with oxidants and H_2S donors (GYY4137 **1** 100 µM; AP39 **3**, 100 nM) as described above and the production of mitochondria-derived generation of reactive oxygen species were determined by fluorimetry using the mitochondria-targeted oxidant probe MitoSox red™ (Invitrogen, 5 µM) and fluorescence determined (RFU) Ex_{390} / Em_{580nm}[43].

3.11 Statistical analysis

All graphs are plotted with mean ± SEM. In all cases, the mean values were calculated from data taken from at least six separate experiments, performed on separate days using freshly prepared reagents. Where significance testing was performed, an independent *t*-test (Student's; two populations) was used; * $P < 0.1$, ** $P < 0.05$, *** $P < 0.01$.

4 Discussion

H_2S has been proposed as novel cytoprotective mediator[22,44-46]. In isolated mesenchymal progenitor cells RNAi-mediated knockdown of CSE potentiated SIN-1, H_2O_2 and 4-HNE-mediated mitochondrial toxicity, an effect reversed with GYY4137[22]. Genetic knockout of CSE renders endothelial[6] and striatal Q111[47] cells more sensitive to oxidative stress-induced toxicity and blood vessels more prone to atherosclerosis[21]. However, it should be noted that this is not seen in all models. For example, hepatocytes from $CSE^{-/-}$ mice exposed to galactosamine/lipopolysaccharide were shown to be more sensitive to oxidative injury than wild type animals[48], although it is unclear if the effects were mediated by H_2S since CSE knock out did not significantly decrease plasma or liver H_2S levels and markedly increased plasma homocysteine levels[48]. Nevertheless, in cell culture experiments, H_2S / HS^- generated from NaSH (albeit at ≥ 100 µM) has been shown to prevent detrimental cytotoxic effects and oxidative protein modification induced by oxidants such as hydrogen peroxide, superoxide, hypochlorite and peroxynitrite (reviewed in reference[46]). In neuronal cells, NaSH (≥ 100 µM) also inhibited oxidative stress-mediated cell death after treatment with β-amyloid[49] or the mitochondrial toxin 1-methyl-4-phenylpyridinium (MPP^+)[50]. Furthermore, H_2S is also reported to inhibit the expression and activity of NAD(P)H oxidase, a key source of extra-mitochondrial oxidant species[51] and it upregulates the expression of the antioxidant enzyme thioredoxin-1 in vascular endothelial cells[52]. However, in each of these studies, the concentrations of H_2S required for each of these studies are often vastly excessive (typically >1-200 µM) and well beyond that seen in health or extreme pathology. Although the absolute level of free H_2S gas in the vasculature is not known, the most recent analytical techniques have suggested levels of free H_2S are in the nM to low µM range, suggesting that many of the above cellular studies using NaSH or Na_2S may not reflect the endogenous effects of physiologically relevant concentrations of H_2S found in the vasculature[2].

We recently showed RNAi-mediated knockdown of CSE rendered mitochondria more sensitive to oxidative stress-induced mitochondrial toxicity, an effect which was overcome by the H_2S donor GYY4137 **1** (albeit ≥100 µM) suggesting that endogenous H_2S may function to preserve mitochondrial integrity[22]. This is supported by *in vivo* studies. For example, in a rodent cardiac ischaemia-reperfusion model, both Na_2S infusion and selective cardiac CSE over-expression preserved mitochondrial ultrastructure,

preserved ATP generation and respiratory chain function *in vivo*[45], possibly *via* a mitochondrial pathway involving the preservation of Bcl-2 signalling, inhibition of Bax, upregulation of PKC and opening of mitochondrial K_{ATP}-channels[10,52].

Collectively, these *in vitro* and *in vivo* studies have strongly suggested that mitochondria are key regulatory targets for endogenous and exogenously applied H_2S suggesting that compounds which deliver H_2S to mitochondria could be therapeutically useful. To test this hypothesis *in vitro,* we exposed microvascular endothelial cells to oxidative insult and examined cell viability and mitochondrial toxicity after oxidative insult using a novel mitochondria-targeted TPP^+-derived dithiolethione (AP39, **3**) and a well established but non-targeted H_2S donor molecule GYY4137 **1**. Concentrations of GYY4137 (100 μM) were chosen based on Figure 3D and the reported cytoprotective effects reported for this compound in a variety of cellular models[14-21]. In each assay (Fig. 3-5), AP39 **3** significantly inhibited oxidative stress induced toxicity at concentrations more than 1,000-fold lower than that of GYY4137 (e.g. 100 nM AP39 *c.f.* 100 μM GYY4137). In contrast, incubation of cells with TPP^+-decanoate (compound **4**) which targets mitochondria, but cannot generate H_2S or the H_2S donor moiety ADT-OH alone (e.g. lacking TPP^+), did not prevent oxidant-induced cell death (Figs. 3A-C). Similarly, incubation of cells with compound **4** and ADT-OH **2** together also failed to show cytoprotective effects indicating that the whole AP39 molecule (e.g. mitochondria-targeted H_2S delivery) was required for cell preservation (Figs 3A-C). Whilst our study clearly shows inhibition of oxidative stress-induced cellular toxicity and mitochondrial preservation by AP39, it is not possible to determine from these data whether mitochondrial protection was the cause or a consequence of cytoprotection. Nevertheless, TPP^--derivatised H_2S donor compounds such as AP39 may be useful tools in studying mitochondria-H_2S interactions.

Although further work is required to define the precise bio-molecular pathways by which AP39 **3** prevents cellular injury, the pathways for endogenous mitochondrial generation of H_2S have recently been uncovered[5,52-56]. The mitochondrial enzyme 3-MST generates low levels of H_2S and 3-MST-derived H_2S concentrations in the nanomolar range were very recently shown to contribute electrons to the Krebs cycle, enhance mitochondrial electron transport and bioenergetics[5], an effect blocked during oxidative stress[54] but reversed with exogenous H_2S[54]. Recently, CSE[53] and CBS[54,55] have been shown to translocate from the cytosol in cells to the mitochondrial matrix in response to hypoxic and calcium stress, to generate H_2S within the mitochondria, possibly acting as an electron acceptor in the mitochondrial respiratory chain, resulting in increased cellular ATP production and cell preservation[53-56]. It is possible that these effects were also mediated by AP39-derived H_2S, contributing to the overall cytoprotective effects of this compound since we observed co-localisation of H_2S generation with mitochondria (Fig. 2B) preservation of ATP levels (Fig. 5B) and mitochondrial $\Delta\psi m$ (Fig. 4A) and decreased mitochondrial oxidant production (Figs. 4B & 5A). Therefore, it appears that the endogenous enzymes responsible for H_2S generation are either located within or translocate to the mitochondria in response to cellular stress and mitochondria-derived H_2S contributes to overall cellular bioenergetics and cellular health. Since mitochondrial production of H_2S is perturbed by oxidative stress and mitochondrial dysfunction and oxidative stress are key pathological events in several human disease states (including hypertension, stroke, neurodegenerative disease, arthritis, hepatitis etc; reviewed in[1-3]), it is likely that mitochondrial H_2S delivery may represent a novel approach to study mitochondrial function in health and disease and potentially reveals a novel therapeutic strategy to treat (or limit) mitochondrial dysfunction in human disease.

5 Conclusions

Our current study shows that coupling H_2S generating diothiolethione (AP39) to a moiety well characterised to enable selective targeting of intracellular mitochondria (TPP^+) greatly increased the cytoprotective potency of H_2S relative to a standard and non-targeted H_2S donor compound GYY4137. Selective pharmacological manipulation of mitochondrial H_2S may represent a novel approach to preserve mitochondrial function and prevent oxidative stress-induced cellular injury *in vivo*.

6 Acknowledgements

The authors are also grateful to the EPSRC National Mass Spectrometry Service Centre (Swansea, UK) for determination of mass spectra and to Ms. Srijana Rai for her technical support.

7 References

1. Wang, R. Physiological implications of hydrogen sulfide: a whiff exploration that blossomed. *Physiol Rev.* **2012**, 971-896

2. Whiteman, M.; Le Trionnaire, S.; Chopra, M.; Fox, B.; Whatmore, J. Emerging role of hydrogen sulfide in health and disease: critical appraisal of biomarkers and pharmacological tools. *Clinical Science* **2011**, 121, 459-488.

3. Vandiver, M. S.; Snyder, S. H. Hydrogen sulfide: a gasotransmitter of clinical relevance. *J. Mol. Med* **2012**, *90*, 255-263.

4. Shibuya N,; Tanaka M,; Yoshida M,; Ogasawara Y, Togawa T,; Ishii K,; Kimura H. 3-Mercaptopyruvate sulfurtransferase produces hydrogen sulfide and bound sulfane sulfur in the brain. *Antioxid. Redox. Signal* **2009**, 11, 701-714.

5. Módis K,; Coletta C,; Erdélyi K,; Papapetropoulos A.; Szabo C. Intramitochondrial hydrogen sulfide production by 3-mercaptopyruvate sulfurtransferase maintains mitochondrial electron flow and supports cellular bioenergetics. *FASEB J.* **2013**, 27, 601-611.

6. Yang, G.; Wu, L.; Jiang, B.; Yang, W.; Qi, J.; Cao, K.; Meng, Q.; Mustafa, A.K.; Mu, W.; Zhang, S.; Snyder, S. H.; Wang, R. H_2S as a physiologic vasorelaxant: hypertension in mice with deletion of cystathionine gamma-lyase. *Science* **2008**, 322, 587-90.

7. Mani, S.; Li, H.; Untereiner, A,; Wu, L.; Yang, G.; Austin, R.C.; Dickhout, J.G.; Lhoták, S.; Meng, Q.H.; Wang, R. Decreased endogenous production of hydrogen sulfide accelerates atherosclerosis. *Circulation* **2013**, 25, 127, 2523-34.

8. Whiteman, M.; Gooding, K.M.; Whatmore, J.L.; Ball, C.I; Mawson, D.; Skinner, K.; Tooke, J.E.; Shore, A.C. Adiposity is a major determinant of plasma levels of the novel vasodilator hydrogen sulphide. *Diabetologia* **2010**, 53, 1722-1726.

9. Wang, K.; Ahmad, S.; Cai, M.; Rennie, J;, Fujisawa, T.; Crispi, F.; Baily, J.; Miller, M.R.; Cudmore, M.; Hadoke, P.W.; Wang, R.; Gratacós, E.; Buhimschi, I.A.; Buhimschi, C.S.; Ahmed, A. Dysregulation of hydrogen sulfide producing enzyme cystationine-γ-lyase contributes to maternal hypertension and placental abnormalities in preeclampsia. *Circulation* **2013**, 127, 2514-2422.

10. Lavu, M.; Bhushan, S.; Lefer, D. J. Hydrogen sulfide-mediated cardioprotection: mechanisms and therapeutic potential. *Clin. Sci.* **2010**, 120, 219-229.

11. Halliwell, B.; Gutteridge, J. Free radicals in biology and

medicine. Oxford University Press, ISBN-10: 019856869X.

12. Murphy, M. P. How mitochondria produce reactive oxygen species. *Biochem J.* **2009**, 417, 1-13.

13. Smith R, A.; Hartley, R. C.; Cocheme, H. M.; Murphy, M. P. Mitochondrial Pharmacology. *Trends Pharmacol. Sci.* **2012**, 341-352.

14. Li, L.; Whiteman, M.; Guan, Y. Y.; Neo, K. L.; Cheng, Y.; Lee, S. W.; Zhao, Y.; Baskar, R.; Tan, C.H.; Moore, P. K. Characterisation of a novel, water-soluble hydrogen sulfide-releasing molecule (GYY4137). New insights into the biology of hydrogen sulfide. *Circulation* **2008**, 117, 2351-2360.

15. Robinson, H.; Wray, S. A new slow releasing, H_2S generating compound, GYY4137 relaxes spontaneous and oxytocin-stimulated contractions of human and rat pregnant myometrium. *PLoS One*. **2012**, 7, e46278.

16. Merighi, S.; Gessi, S.; Varani, K.; Fazzi, D.; Borea, P.A. Hydrogen sulfide modulates the release of nitric oxide and VEGF in human keratinocytes. *Pharmacol. Res*. **2012** 66, 428-436.

17. Perry, M.M.; Hui, C.K.; Whiteman, M.; Wood, M.E.; Adcock, I.; Kirkham, P.; Michaeloudes, C.; Chung, K.F. Hydrogen sulfide inhibits proliferation and release of IL-8 from human airway smooth muscle cells. *Am. J. Respir. Cell. Mol. Biol*. **2011**, 45, 746-752.

18. Li, L.; Salto-Tellez, M.; Tan, C. H.; Whiteman, M.; Moore, P.K. GYY4137, a novel ; hydrogen sulfide-releasing molecule, protects against endotoxic shock in the rat. *Free Radic. Biol. Med*. **2009**, 47, 103-113.

19. Whiteman, M.; Li, L.; Rose, P.; Tan, C.H.; Parkinson, D.B.; Moore, P.K. The effect of hydrogen sulfide donors on lipopolysaccharide-induced formation of inflammatory mediators in macrophages. *Antioxid. Redox. Signal*. **2010**,12, 1147-1154.

20. Li, L.; Fox, B.; Keeble, J.; Salto-Tellez, M.; Winyard, P.G.; Wood, M.E.; Moore, P.K. Whiteman M. The complex effects of the slow-releasing hydrogen sulfide donor GYY4137 in a model of acute joint inflammation and in human cartilage cells. *J Cell. Mol. Med.* **2013**, 17, 365-376.

21. Liu, Z.; Han, Y.; Li, L.; Lu, H.; Meng, G.; Li, X.; Shirhan, M.; Peh, M.T.; Xie, L.; Zhou, S.; Wang, X.; Chen, Q.; Dai, W.; Tan, C.H.; Pan, S.; Moore, P.K.; Ji, Y. The hydrogen sulfide donor, GYY4137, exhibits anti-atherosclerotic activity in high fat fed apolipoprotein E(-/-) mice. *Br. J. Pharmacol*. **2013**,169, 1795-1809.

22. Fox, B,; Schantz, J-T,; Haigh, R.; Wood, M.E,; Moore, P.K,; Viner, N.; Spencer, J.P.; Winyard, P.G., Whiteman, M.; Inducible hydrogen sulfide synthesis in chondrocytes and mesenchymal progenitor cells: is H_2S a novel cytoprotective mediator in the inflamed joint? *J Cell. Mol. Med*. **2012**, 16, 896-910.

23. Caliendo, G.; Cirino, G.; Santagada, V.; Wallace, J.L. Synthesis and biological effects of hydrogen sulfide (H_2S): development of H_2S-releasing drugs as pharmaceuticals. *J Med. Chem.* **2010**, 53, 6275-6286.

24. Wood, M.E.; Whiteman, M.; Perry, A. Hydrogen sulfide releasing compounds and their use. *Patent application* WO2013045951.

25. Wallace, J. L. Hydrogen sulfide: a rescue molecule for mucosal defence and repair. *Dig. Dis. Sci.* **2012**, 57, 1432-1434.

26. Li, L.; Rossoni, G.; Sparatore, A.; Lee, L.C.; Del Soldato, P.; Moore, P. K. Anti-inflammatory and gastrointestinal effects of a novel diclofenac derivative. *Free Radic. Biol. Med*. **2007**, 42, 706-719.

27. Chan, M. V.; Wallace, J. L. Hydrogen sulfide-based tharapeutics and gastrointestinal disease: Translating physiology to treatments. *Am. J. Physiol. Gastrointest. Liver Physiol.* **2013**, 305, G467-473.

28. Campolo, M.; Esposito, E.; Ahmad, A.; Di Paola, R.; Wallace, J. L. Cuzzocrea S. A hydrogen sulfide-releasing cyclooxygenase inhibitor markedly accelerates recovery from experimental spinal cord injury. *FASEB J*. **2013**, 27, 4489-4499.

29. Liu, C.; Pan, J.; Li, S.; Zhao, Y.; Wu, L.Y.; Berkman, C.E.; Whorton, A.R.; Xian, M. Capture and visualization of hydrogen sulfide by a fluorescent probe. *Angew Chem. Int. Ed. Engl*. **2011**, 50, 10327-10329.

30. Cortese-Krott, M.M.; Fernandez, B.O.; Santos, J.L.; Mergia, E.; Grman, M.; Nagy, P.; Kelm, M.; Butler, A.; Feelisch, M. Nitrosopersulfide (SSNO(-)) accounts for sustained NO bioactivity of S-nitrosothiols following reaction with sulfide. *Redox Biol*. **2014**, 2, 234-244.

31. Thorson, M.K.; Majtan, T.; Kraus, J.P.; Barrios, A.M. Identification of cystathionine β-synthase inhibitors using a hydrogen sulfide selective probe. *Angew Chem. Int. Ed. Engl*. **2013**, 52, 4641-4644.

32. Chen, B.; Li, W.; Lv, C.; Zhao, M.; Jin, H.; Du, J.; Zhang, L.; Tang, X. Fluorescent probe for highly selective and sensitive detection of hydrogen sulfide in living cells and cardiac tissues. *Analyst* **138**, 946-951.

33. Thurnhofer, S.; Vetter, W. Synthesis of *(S)*-(+)-enantiomers of food-relevant (*n*-5)-monoenoic acid saturated anteiso-fatty acids by a Wittig reaction. *Tetrahedron* **2007**, 63, 1140-1145.

34. Ohtsuki, S.; Ikeda, C.; Uchida, Y.; Sakamoto, Y.; Miller, F.; Glacial, F.; Decleves, X.; Scherrmann, J.M.; Couraud, P.O.; Kubo, Y.; Tachikawa, M.; Terasaki, T. Quantitative targeted absolute proteomic analysis of transporters, receptors and junction proteins for validation of human cerebral microvascular endothelial cell line hCMEC/D3 as a human blood-brain barrier model. *Mol Pharm*. **2013**, 10, 289-296.

35. Mkrtchyan H,; Scheler, S.; Klein, I.; Fahr, A.; Couraud. P.O.; Romero, I. A.; Weksler, B.; Liehr, T. Molecular cytogenetic characterization of the human cerebral microvessel endothelial cell line hCMEC/D3. *Cytogenet. Genome Res*. **2009**, 126, 313-317.

36. Weksler, B.; Romero I. A., Couraud, D. The hCMEC/D3 cell line as a model for the human blood brain barrier. *Fluids Barriers CNS*, **2013**, 10, 16.

37. Watanabe, T.; Dohgu, S.; Takata, F.; Nishioku, T.; Nakashima, A.; Futagami, K.; Yamauchi, A.; Kataoka, Y. Paracellular barrier and tight junction protein expression in the immortalized brain endothelial cell lines bEND.3, bEND.5 and mouse brain endothelial cell 4. *Biol. Pharm. Bull*. **2013**, 36, 492-495.

38. Park, T.Y.; Baik. E.J.; Lee. S.H. Prostaglandin E_2-induced intercellular adhesion molecule-1 expression is mediated by cAMP/Epac signalling modules in bEnd.3 brain endothelial cells. *Br. J. Pharmacol*. **2013**, 169, 604-618.

39. Davidson, S.M.; Duchen, M.R. Endothelia Mitochondria: Contributing to vascular function and disease. *Circ. Res.* **2007**, 100, 1128-1141.

40. Cai, H.; Harrison, D.G. Endothelial dysfunction in cardiovascular disease: The role of oxidative stress. *Circ. Res.* **2000**, 87, 840-844.

41. Whiteman, M.; Armstrong, J. S.; Cheung, N. S.; Siau, J.L.;

Rose, P.; Schantz, J-T.; Jones, D. P.; Halliwell, B. Peroxynitrite mediates calcium-dependent mitochondrial dysfunction and cell death via activation of calpains. *FASEB J.* **2004**, 18, 1395-1397.

42. Whiteman, M.; Rose, P.; Siau, J.L.; Cheung, N. S.; Tan, G. S.; Halliwell, B.; Armstrong, J. S. Hypochlorous acid induced mitochondrial dysfunction and apoptosis in human hepatoma HepG2 and fetal liver cells: role of mitochondrial permeability transition. *Free Radic. Biol. Med.* **2005**, 38, 1571-1584.

43. Robinson, K.M.; Janes, M.S.; Pehar, M.; Monette, J.S.; Ross, M.F.; Hagen, T.M.; Murphy, M.P.; Beckman, J.S. Selective fluorescent imaging of superoxide in vivo using ethidium based probes. *Proc. Natl. Acad. Sci. USA.* **2006**, 103, 15038-15043.

44. Suzuki, K.; Olah, G.; Modis, K.; Coletta, C.; Kulp, G.; Gerö, D.; Szoleczky, P.; Chang, T.; Zhou, Z.; Wu, L.; Wang, R.; Papapetropoulos, A.; Szabo C. Hydrogen sulfide replacement therapy protects the vascular endothelium in hyperglycemia by preserving mitochondrial function. *Proc. Natl. Acad. Sci.U SA.* **2011,** 108, 13829-13834.

45. Kondo, K.; Bhushan, S.; King, A.L.; Prabhu, S.D.; Hamid, T.; Koenig, S.; Murohara, T.; Predmore, B.L.; Gojon, G. Sr.; Gojon, G.; Wang, R.; Karusula, N.; Nicholson, C.K.; Calvert, J.W.; Lefer, D.J. H_2S protects against pressure overload induced heart failure via upregulation of endothelial nitric oxide synthase. *Circulation*. **2013**, 127, 1116-1127

46. Whiteman, M.; Moore, P. K. Hydrogen sulfide and the vasculature: a novel vasculoprotective entity and regulator of nitric oxide bioavailability? *J. Cell. Mol. Med.* **2009**, 13, 488-507.

47. Paul, B.D.; Sbodio, J.I.; Xu, R.; Vandiver, M.S.;Cha, J.Y.; Snowman, A. M.; Snyder, S.H. Cystathione-γ-lyase deficiency mediates neurodegeneration in Huntingdon's disease. *Nature* **2014**, doi:10.1038/nature13136.

48. Shirozu, K.; Tokuda, K.; Marutani, E,; Leferm D,; Wangm R.; Ichinose, F. Cystathionine γ-lyase deficiency protects mice from galactosamine/lipopolysaccharide-induced acute liver failure. *Antioxid Redox Signal*. **2014**, 20, 204-216.

49. Liu, Y. Y.; Bian, J. S. Hydrogen sulfide protects amyloid-β induced cell toxicity in microglia. *J. Alzheimers Dis.* **2010**, 22, 1189-1200.

50. Yin, W.L.; He, J.Q.; Hu, B.; Jiang, Z.S.; Tang, X. Q. Hydrogen sulfide inhibits MPP(+)-induced apoptosis in PC12 cells. *Life Sci.* **2009**, 269-275.

51. Xu Z S.; Wang, X.Y.; Xiao, D.M.; Hu, L.F.; Lu, M.; Wu, Z.Y.; Bian, J.S. Hydrogen sulfide protects MC3T3-E1 osteoblastic cells against H_2O_2-induced oxidative damage-implications for the treatment of osteoporosis. *Free Radic. Biol. Med*. **2011**, 50, 314-323.

52. Vacek, T. P.; Gillespie, W.; Tyagi, N.; Vacek, J. C.; Tyagi, S. C. Hydrogen sulfide protects against vascular remodeling from endothelial damage. *Amino Acids* **2010**, 39, 1161-1169.

53. Fu, M.; Zhang, W.; Wu, L.; Yang, G.; Li, H.; Wang, R. Hydrogen sulfide (H_2S) metabolism in mitochondria and its regulatory role in energy production. *Proc. Natl. Acad. Sci. USA*. **2012**, 109, 2943-2948.

54. Módis, K.; Asimakopoulou, A.; Coletta, C.; Papapetropoulos, A.; Szabo, C. Oxidative stress suppresses the cellular bioenergetic effect of the 3-mercaptopyruvate sulfurtransferase/hydrogen sulfide pathway. *Biochem. Biophys. Res. Commun*. **2013**, 433, 401-407.

55. Szabo, C.; Coletta, C.; Chao, C.; Módis, K.; Szczesny, B.; Papapetropoulos, A.; Hellmich, M.R. Tumor-derived hydrogen sulfide, produced by cystathionine-β-synthase, stimulates bioenergetics, cell proliferation, and angiogenesis in colon cancer. *Proc. Natl. Acad. Sci. USA*. **2013**, 110, 12474-12479.

56. Teng, H.; Wu, B.; Zhao, K.; Yang, G.; Wu, L.; Wang, R. Oxygen-sensitive mitochondrial accumulation of cystathionine β-synthase mediated by Lon protease. *Proc. Natl. Acad. Sci. USA*. **2013**, 110, 12679-12684.

8 Notes

Corresponding authors:
*[a] *University of Exeter Medical School, St. Luke's Campus, Magdalen Road, Exeter EX1 2LU, England, Tel: +44(0)1392 722942; E-mail: m.whiteman@exeter.ac.uk*
*[b] *Biosciences, College of Environmental and Life Sciences, University of Exeter, Geoffrey Pope Building, Stocker Road, Exeter EX4 4QD,* England *Tel: +44(0)1392 723450; E-mail: m.e.wood@exeter.ac.uk*